Title: Catalytic conversion of glucose to 5-hydroxymethylfurfural over biomass-based activated carbon catalyst

Authors: Annu Rusanen, Riikka Lahti, Katja Lappalainen, Johanna Kärkkäinen, Tao Hu, Henrik Romar, Ulla Lassi

PII: S0920-5861(18)31324-5
DOI: https://doi.org/10.1016/j.cattod.2019.02.040
Reference: CATTOD 11992

To appear in: *Catalysis Today*

Received date: 27 September 2018
Revised date: 10 January 2019
Accepted date: 16 February 2019

Please cite this article as: Rusanen A, Lahti R, Lappalainen K, Kärkkäinen J, Hu T, Romar H, Lassi U, Catalytic conversion of glucose to 5-hydroxymethylfurfural over biomass-based activated carbon catalyst, *Catalysis Today* (2019), https://doi.org/10.1016/j.cattod.2019.02.040

Catalytic conversion of glucose to 5-hydroxymethylfurfural over biomass-based activated carbon catalyst

Annu Rusanen[a], Riikka Lahti[a,b], Katja Lappalainen[a,b], Johanna Kärkkäinen[a], Tao Hu[a], Henrik Romar[a], Ulla Lassi*[,a,b]

[a] University of Oulu, Research Unit of Sustainable Chemistry, P.O. Box 4300, FIN-90014 Oulu, Finland
[b] University of Jyväskylä, Kokkola University Consortium Chydenius, Talonpojankatu 2B, FIN-67100 Kokkola, Finland

*Corresponding author: ulla.lassi@oulu.fi

Graphical abstract

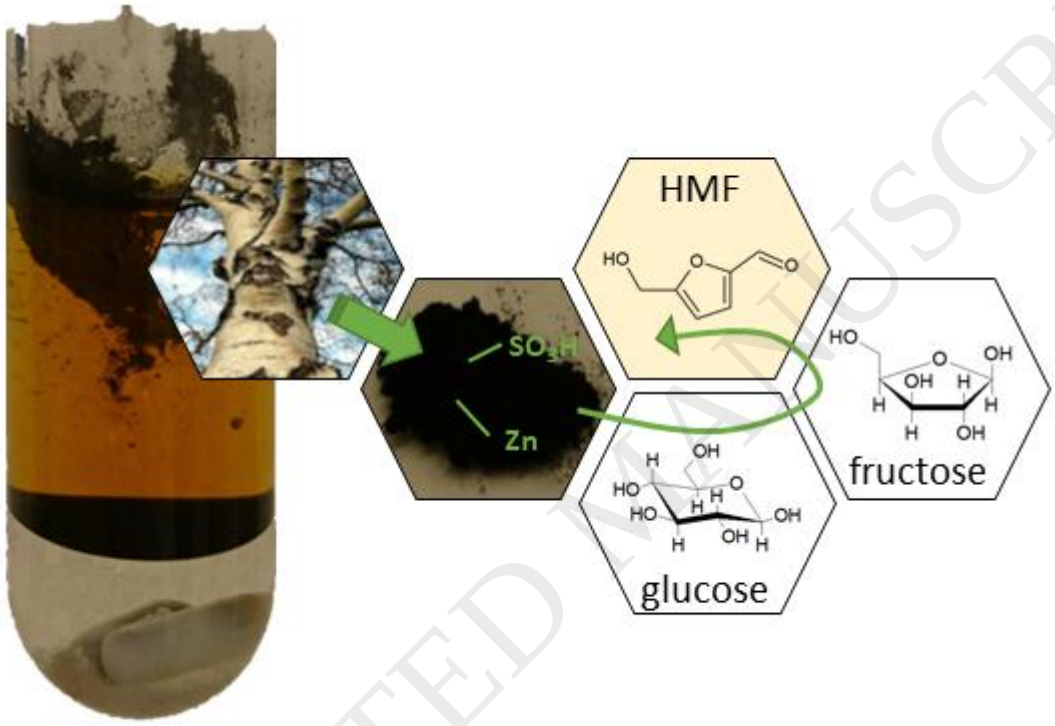

Highlights

- Biomass-based activated carbon catalysts modified with Lewis or Brønsted acid sites were prepared
- Catalysts were used to convert glucose to HMF in biphasic water:THF system
- 51% HMF yield was obtained with catalytic mixture containing both Lewis and Brønsted acid sites
- The water phase containing the catalyst was recycled successfully

Abstract

Selective and efficient dehydration of glucose to 5-hydroxymethylfurfural (HMF) has been widely explored research problem recently, especially from the perspective of more sustainable heterogeneous catalysts. In this study, activated carbon was first produced from a lignocellulosic waste material, birch sawdust. Novel heterogeneous catalysts were then prepared from activated carbon by adding Lewis or Brønsted acid sites on the carbon surface. Prepared catalysts were used to convert glucose to HMF in biphasic water:THF

system at 160 °C. The highest HMF yield and selectivity, 51% and 78%, respectively, were obtained in 8 hours with a catalytic mixture containing both Lewis and Brønsted acid sites. Also, preliminary recycling experiments were performed. Based on this study, biomass-based activated carbon catalysts show promise for the conversion of glucose to HMF.

Keywords
Activated carbon; Catalyst; 5-hydroxymethylfurfural; Glucose conversion

1. Introduction

The limitations of fossil resources have driven global society toward bioeconomy, in which bioresources are utilized in the production of biofuels and biochemicals. 5-hydroxymethylfurfural (HMF), a top value-added biomass-derived chemical, has emerged as an important target product, since it represents a potential substitute for petroleum-based monomers of various polymers and can be used as a starting material for biofuels, solvents, and pharmaceuticals [1, 2]. HMF is a heterocyclic furanic molecule substituted in 2–5 positions with hydroxide and aldehyde functionalities (Figure 1), making it capable oxidizing into a dicarboxylic acid or reducing to a diol, both of which can be used for the synthesis of polymers. In addition, as a relatively unsaturated aromatic compound, HMF can be upgraded to a fuel *via* hydrogenation, and the heterocyclic structure of furans can be found in an array of biologically active molecules with pharmaceutical applications. [3]

HMF can be produced by the dehydration of C6 carbohydrates, including monomeric and polymeric carbohydrates, such as fructose, glucose, sucrose, starch, cellulose, and raw biomass. The mechanistic pathway of transformation is not yet clear, although a few possible alternatives have been proposed [4]. The most widely discussed route, when using fructose as feedstock, is direct dehydration of hexoses into HMF, *via* either an acyclic or cyclic intermediate [5, 6]. When using hexoses other than fructose, isomerization has been proposed as an initial step prior to dehydration (Figure 1) [4]. Because of this extra step, the typical yields of HMF from fructose are superior to those obtained from glucose or other hexoses under the same reaction conditions. Up to 99% yields have already been achieved in fructose conversion to HMF [7]. Still, it should be emphasized that fructose is not an ideal feedstock because of its high price and low abundance in nature [8]. It exists only in food biomass, such as in sugar cane or corn; in contrast, glucose is the cheapest hexose and the most abundant monosaccharide, and is also available in non-food lignocellulosic biomass. Therefore, the conversion of glucose to HMF is an important challenge worthy of study.

There are many ways to produce HMF from glucose—for example, aqueous, organic, biphasic and ionic liquid systems have all been utilized recently [4]. When compared to fructose conversion systems, the challenge with glucose conversion is to find media wherein a rather stable glucose pyranose can transfer effectively into a furanose form. Also, the low selectivity of the dehydration reaction, which is caused by multiple side reactions, such as the formation of undesired byproducts, lowers the yield [9]. Formic acid and levulinic acid can be formed *via* the rehydration of HMF [10]. Also, a cross-polymerization reaction leads to the formation of soluble polymers and insoluble brown humins [11]. Biphasic systems are promising media for conversion since the separation of HMF is simple and the system is recyclable, while yields remain good (up to 81% in THF/water/NaCl system) [12, 13]. The most remarkable advantage of the biphasic system is the continuous removal of HMF from the reaction mixture, which prevents rehydration

reactions and increases yields. DMSO:water, MIBK:water, and THF:water are the most-used biphasic systems according to the literature [4, 14].

In addition to reaction media, the catalyst also plays an important role in reaction selectivity and the dehydration rate. The dehydration step is generally catalyzed by mineral or organic acid. The catalyst should either possess a proton or be a Lewis acid [15, 16]. The most commonly used Brønsted acids are sulfuric acid, phosphoric acid, hydrochloric acid, oxalic acid, levulinic acid, and p-toluenesulfonic acid [4]. The isomerization step is catalyzed by Brønsted bases or Lewis acids [17]. However, the basic catalyst typically leads to side reactions, so Lewis acids, such as metal chlorides, are favored [18]. Homogeneous metal chlorides are capable of producing good HMF yields from glucose, e.g., $AlCl_3$ produced a 61% yield in the biphasic system at 160 °C [19]. Also, tandem systems, in which the presence of both Lewis and Brønsted acidity are combined, have been used, e.g., $AlCl_3$ and HCl as a tandem system produced a 62% yield in the biphasic system at 170 °C [20].

However, traditional homogeneous catalysts are not easily recycled, they cause corrosion and incur significant costs in separation and waste treatment processes. Heterogeneous catalysts, on the other hand, are easily separated from the liquid reaction mixture after the reaction, enabling their reuse. Therefore, the replacement of homogeneous catalysts with heterogeneous catalysts is preferred and is currently drawing attention in the research field [21]. The most commonly used heterogeneous acid catalysts include metal oxides, functional polymers, ion exchange resins, and zeolites [22-25]. As an alternative to them, novel heterogeneous catalysts can be prepared from activated carbons (AC). ACs are low-cost materials possessing large specific surface areas, well-developed, highly porous structures, chemical and physical stability, and surface functionalities influencing the surface characteristics and adsorption behavior. ACs can be inert or active in reactions. The carbon materials exhibit an acid–base character by containing heteroatom, such as oxygen-bearing surface groups, which can have an effect on its properties. [26-29] Furthermore, AC can be used as a catalyst support and be chemically functionalized and/or impregnated with metals to improve catalytic activity [30-32]. ACs can be prepared from any carbon-containing raw material, including bituminous coal and lignite, from which a large part of the ACs on the market is produced [33]. Biomass-based ACs [34-36] are becoming more attractive, since they can be prepared from lignocellulosic second-generation biomasses, side streams, and waste materials as a renewable raw material, and as such contribute to carbon neutrality in the face of climate change.

Recently, a few studies have been published about fructose conversion to HMF by using modified carbon catalysts: Deng et. al. used sodium ligninsulfonate derived AC as a catalyst support functionalized with phosphoric acid, whereas Xiong et. al. used wood-based forestry biochar sulfonated with sulfuric acid [37, 38]. Both studies generated good HMF yields, —55.6% and 42.3%, respectively—using water as a conversion solvent. In addition, other studies have used glucose as a feedstock: Zou et al. used bagasse-based activated carbon and sulfonated it with sulfuric acid, while Villanueva et al. used carboxylated activated carbon [39, 40]. However, both studies produced low HMF yields: 10%, at 130 °C in 8 hours; and < 5%, at 125 °C in 3 hours, respectively. Meanwhile, Tyagi et al. combined Brønsted and Lewis acid sites in the same carbon catalyst by impregnating metals into sulfuric acid-treated activated carbon [41]. These researchers were able to produce a 49% HMF yield using cellulose as feedstock and an ionic liquid as a reaction medium. In this work, AC produced from birch sawdust was modified with $ZnCl_2$ or H_2SO_4 to create Lewis or Brønsted acid sites, respectively, on the AC surface. The objective was then to study the effectiveness of prepared heterogeneous AC catalysts in the conversion of glucose to HMF in biphasic water:THF system. The reaction conditions were studied in detail to find optimal catalyst loading and reaction time. Furthermore, the recyclability of the catalyst containing water phase was studied with some preliminary experiments.

Figure 1. General reaction scheme of HMF formation from glucose. First, glucose is isomerized into fructose over a Lewis acid catalyst, and then fructose is dehydrated into HMF over a Brønsted acid catalyst.

2. Experimental

2.1 Materials

All chemicals in this work were commercially available and were used without further purification. Birch sawdust (*Betula pendula*) was received from a sawmill in Northern Sweden.

2.2 Activated carbon support and catalyst preparation

Activated carbon was produced from birch sawdust. The sawdust was dried, carbonized and steam-activated in a one-step process in a rotating quartz reactor (Nabertherm GmbH RSRB 80). The thermal profile during the process was divided into two parts. In the carbonization step, which was performed under an N_2 flow (200 ml/min), the temperature was raised to 800 °C with a ramp of 6.7 °C/min. During the activation, the temperature was kept at 800 °C for 120 minutes with a stream of water steam and N_2 gas (120 g/h at 140 °C and 200 ml/min, respectively). The resulting activated carbon (AC, Figure 2) was crushed and sieved to a fraction size of < 150 µm. Finally, it was either washed with hot water (ACW, Figure 2) or used as such for further modification.

Modified solid acid catalysts were prepared by the reflux method from AC or the impregnation method from ACW. To introduce Brønsted acid sites on the activated carbon surface, untreated AC was heated in reflux system at 80 °C for 2 hours with 9 M or 18 M H_2SO_4 (ACB or ACB2, Figure 2). The amount of acid was 10 mL per g of AC. After acid treatment, ACBs were filtered and washed with distilled water until the pH of the filtrate was neutral; lastly, the ACBs were dried overnight at 105 ˚C. Dried ACBs were extracted in boiling toluene for 2 hours in order to remove unreacted sulfuric acid, after which they were water-washed and then dried overnight at 105 ˚C [42]. To introduce Lewis acid sites on the ACW surface, catalysts were prepared by incipient-wetness impregnation method [43-44] of a precursor salt, $ZnCl_2$, and selected to contain nominal 5 wt.% or 15 wt.% of zinc (ACL and ACL2, respectively, Figure 2). Impregnation was performed overnight in a rotating mixer (Rotavapor) at room temperature. After impregnation, the catalysts were dried overnight at 105 °C. The thermal calcination treatment was performed in a chemical vapor deposition (CVD) oven at 550 °C for 2.5 hours with an N_2 flow (240 ml/h per g of catalyst). In addition, two catalytic mixtures, ACBL and ACBL2, were made by combining equal amounts of ACB and ACL or ACB2 and ACL2, respectively (Figure 2).

Figure 2. Flow chart for catalyst preparation: a) carbonization and activation step b) acid modification with 9 M H_2SO_4 c) acid modification with 18 M H_2SO_4 d) washing with H_2O e) impregnation with $ZnCl_2$ (5 wt.% Zn) f) impregnation with $ZnCl_2$ (15 wt.% Zn) g) mixing in 1:1 ratio.

2.3 Characterization of catalysts

The morphology of the catalyst particles was studied using a JEOL JEM-2200FS energy filtered transmission electron microscope equipped with a scan generator (EFTEM/STEM). The catalyst samples were dispersed in pure ethanol and pretreated in an ultrasonic bath for several minutes to create a microemulsion. A small drop of the microemulsion was deposited on a copper grid pre-coated with carbon (Lacey/Carbon 200 Mesh Copper) and evaporated in air at room temperature. The accelerating voltage in the measurements was 200 kV, while the resolution of the STEM image was 0.2 nm. The metal particle sizes were estimated from high-resolution STEM images of each sample.

Specific surface areas were calculated from adsorption isotherms of N_2 at isothermal conditions in liquid nitrogen according to the Brunauer–Emmett–Teller (BET) theory [45]. Pore distribution was calculated from the adsorption isotherms using the density functional theory (DFT) model [46]. The fresh catalyst samples (about 100 mg) were weighted in a quartz tube. Samples were evacuated and heated to 140 °C to remove any adsorbed components as well as to reduce moisture. The measurements were performed by a Micromeritics ASAP 2020 equipment.

The Zn, Na, K, Ca, and S contents of prepared AC and catalysts were measured by ICP-OES using a Perkin Elmer Optima 5300 DV instrument. Samples of 0.1-0.2 g were first digested in a microwave oven (MARS, CEM Corporation) with 9 ml of HNO_3 at 200 °C for 10 minutes. Then, 3 ml of HCl was added, and the mixture was digested at 200 °C for 10 minutes. Finally, 1 ml of HF was added, and the mixture was again digested at 200 °C for 10 minutes. Excess HF was neutralized with H_3BO_3 by heating at 170 °C for 10 minutes. Afterwards, the solution was diluted to 50 ml with water, and the former elements were analyzed by the ICP-OES.

X-ray diffractograms were recorded by Rigaku SmartLab 9 kW X-ray diffraction (XRD) equipment using Cu K_α radiation (K_β filtered) at 45 kV and 200 mA. Diffractograms were collected in the 2θ range of 5–100°, with a step size of 0.02° and a scan speed of 4.06 degree/min. The crystalline phases and structures were analyzed by PDXL2 program and PDF-4^+ 2018.

X-ray photoelectron spectroscopy (XPS) analyses were performed using the Thermo Fisher Scientific ESCALAB 250Xi XPS System. With a pass energy of 20 eV and a spot size of 900 µm, the accuracy of the reported binding energies (BEs) was ±0.2 eV. The Zn, C, O, S, and N were measured for all samples. The measurement data were analyzed by Avantage software. The monochromatic AlKα radiation (1486.6 eV) was operated at 20 mA and 15 kV. Charge compensation of the BEs was performed by applying the C1s line at 284.8 eV as a reference.

Temperature programmed desorption (TPD) of NH_3 was performed by an AutoChem II 2920 system. Prior to the NH_3-TPD analysis, the samples (about 100 mg) were pre-treated in an He flow of 50 ml/min at 600 °C for 30 minutes. Afterward, the samples were cooled to 100 °C, and the adsorption of ammonia (50 ml/min of 15% NH_3/He at 100 °C) was continued for 60 minutes. Prior to the desorption, the samples were flushed in an He flow of 50 ml/min for 30 minutes to remove all reversibly adsorbed NH_3. The NH_3 desorption was carried out from 100 to 800 °C and left for 10 minutes at this temperature. During the analysis, a temperature ramp of 10 °C/min and an He flow rate of 50 ml/min were used. The total amount of acid sites (mmol/g) were calculated.

2.4 Conversion of glucose into HMF

In a typical reaction, 45 mg (0.25 mmol) of glucose, 0.35 g of NaCl, 1.5-18 mg of catalyst (corresponding to 0.4-5.0 µmol of Zn and 0.7-23 mM H_2SO_4), and a magnetic stirring bar were placed into a 5 ml reaction tube. Water (1 ml) and THF (3 ml) were added, and the tube was sealed. The reaction was carried out in a Biotage Initiator microwave reactor at 160 °C for 30 minutes to 8 hours. After the reaction, a sample was taken from both phases, which were filtered through a 0.45 µm PTFE filter for further analysis. The pH of the water phase was checked before and after the reaction. In the recycling experiments, the organic phase was removed after the reaction, and a new portion of glucose and THF was added to a recycled water phase, which included the catalyst. Recycling continued for five runs. All reactions were duplicated.

2.5 Analytical methods

High-performance liquid chromatography (HPLC) and gas chromatography (GC) were used as analytical methods to determine the amount of HMF in the reaction solutions. The water phase was analyzed with HPLC, while the organic phase was analyzed with HPLC and GC. HPLC analysis was carried out using a Waters 2695 separation module fitted with an Atlantis T3 (3 µm, 4.6 x 150 mm) column and a Waters 996 photodiode array (PDA) detector. A water:methanol (90:10) mixture was used as the mobile phase, with a flow rate of 1 ml/min. The injection volume was 4 µl. The column temperature was kept constant at 30 °C, and the UV detection for HMF was performed at 284 nm. GC analysis was carried out using an HP 6890 Series GC system fitted with a Sulpelco SPB-1701 (0.25 µm, 15 m x 0.25 mm) column and an HP 5973 mass selective detector. The oven temperature program was as follows: from 60 °C (hold 1 min) at 20 °C/min to 250 °C (hold 2 min), with the injection and detection temperatures set at 250 °C. Helium was used as a carrier gas, with a flow of 1.5 ml/min. GC-MS was also used to qualitatively determine the byproducts of the conversion reaction. Amounts of byproducts other than levulinic acid were not determined. HMF and LA calibrations were performed using analytical standards (Sigma Aldrich).

The yield of HMF was calculated from the equation:
Y_{HMF} (%) = [concentration of HMF in the sample / theorethical maximum concentration of HMF in the sample] x 100%

The yield of LA was calculated using the same principle.

To determine the reaction selectivity, the amount of glucose from water phase was measured after the conversion reaction. Glucose was measured with YSI 2700 Select Biochemistry Analyzer with glucose solution (2.5 g/l) as a standard. The selectivity of HMF production was then calculated using the following equation:
Selectivity (%) = [moles of HMF produced / (moles of glucose at the beginning - moles of glucose after the reaction)] x 100%

3. Results and discussion

3.1 Characterization of catalysts

AC catalysts prepared in this work were ACW, two Lewis acid catalysts (ACL and ACL2), and two Brønsted acid catalysts (ACB and ACB2). Prepared catalysts were characterized with multiple characterization

techniques to verify their catalytic composition, morphology, and surface properties, e.g., surface areas, active metal phases, and functional groups.

Catalyst morphology was observed with transmission electron microscope (EFTEM/STEM). From STEM images (Fig. S1), no major differences in the surface composition were detected when the ACW surface was compared to the surfaces of ACB and ACB2. Instead, on Lewis acid catalysts (ACL and ACL2) prepared from $ZnCl_2$, metal particles were clearly seen and evenly distributed on the surface of the catalyst. Metal particle sizes in both ACL and ACL2 catalyst were ca. 10–50 nm; however, some metal aggregations around 100 nm were also detected on both catalysts.

Specific BET surface areas, average pore volumes, and pore size distributions of the prepared AC support and catalysts were calculated from nitrogen adsorption isotherms by the BET and DFT methods (Table S1). AC had a BET surface area of 800 m^2/g. The pore volumes were ca. 0.5 cm^3/g with mesopore (2–50 nm) volumes of 52% according to the DFT model. Moreover, all catalysts had high BET surface areas, from 560 to 860 m^2/g, with high mesoporous volumes, which are usually preferred in catalytic systems. The mesoporous structure was preferred, since smaller pores can easily be blocked, especially in the liquid phase. Chemical modification of the AC support with concentrated sulfuric acid seemed to have an impact on the surface pore composition. The treatment opened mesoporous structure of the AC surface. Therefore, there was a 20% increase in the mesopore volumes and a decrease in micropore volumes in ACB2 compared to AC. As the result, the surface area decreased to 700 m^2/g (Table S1). When AC was treated with 9 M H_2SO_4, both surface area and meso and micropore volumes decreased (ACB, Table S1). This might be due to some pore blocking or the addition of functional groups into the pores. To prepare ACW catalyst AC was washed with water, which did not alter the surface area or the meso and micropore volumes considerably (Table S1). However, when ACW was further impregnated with zinc precursor, the surface areas and pore volumes decreased slightly, ca. 3-5% compared to ACW (ACL and ACL2, Table S1). This indicated that metal was present in the pores and surfaces of the ACL and ACL2 catalysts.

The Zn and S contents of the ACW, ACB, ACB2, ACL and ACL2 catalysts were measured with ICP-OES. The nominal active metal contents in ACL and ACL2 were 5 or 15 wt.% of Zn, respectively. However, their Zn contents measured by ICP-OES were similar, 1.7 wt.% for ACL and 1.8 wt.% for ACL2. Therefore, the detected zinc concentrations in catalysts ACL and ACL2 were lower than nominal. It has been proposed in literature that during the heat treatment process, in the temperature range between 400-600 °C, the $ZnCl_2$ dissociates to Zn and Cl_2. Therefore, the evaporation of Zn and Cl_2 could have occurred, though the temperature was below the boiling point of $ZnCl_2$ (b.p.732°C) [47]. Further, reaction of $ZnCl_2$ into ZnO in the presence of oxygen can occur [47, 48]. Since no O_2 was present in the inert atmosphere (N_2) of calcination process, it is possible that Zn was bonded only with the oxygen atoms on the surface of AC. No zinc was detected in ACB and ACB2 catalysts, however, sulfur was present 0.37 wt.% (ACB) or 0.24 wt.% (ACB2) indicating the addition of sulfur during the H_2SO_4 treatment. In all catalysts, other impurity metals, e.g., K, Na, were present in negligible amounts (< 0.2 wt.%). Although some calcium was detected from the ACL catalysts (< 1 wt.%), in ACBs it was present in negligible amounts (< 0.2 wt.%).

Metal phases in the catalysts were observed with XRD (Fig. S2). In all catalysts, the assignments from carbon (JCPDS file no. 01-082-9929) were detected at 2θ=24.6° and 2θ=43.7°, with broad peaks indicating the amorphous phase of the carbon. For AC, ACW, ACB, ACL, and ACL2, phase identification was detected for polymorphic silica (tridymite, SiO_2) according to JCPDS file no. 04-012-1133, with peaks at 2θ=20.5, 21.6, 23.2, 29.9, and 35.8°. In ACB2, no silica was detected with XRD analysis. This indicates that the treatment with 18 M H_2SO_4 removes most of the metal impurities (e.g., water-soluble metals and silica originating from biomass) from AC, since no peaks other than the one for carbon were detected from the ACB2. This was also verified with ICP-OES analysis. For the Lewis acid catalysts, ACL and ACL2, JCPDS file no.

04-004-4531 presented zinc oxide corresponding to ZnO(100), (002), (101), (102), (110), (103), and (112), with peaks at 2θ=31.7, 34.4, 36.2, 47.5, 56.6, 62.8, and 68.0°, respectively. No $ZnCl_2$ or metallic Zn^0 was detected, which confirms that $ZnCl_2$ was decomposed or bonded to the oxygen functionalities on the catalyst surface.

XPS was performed to determine the presence and abundance of oxygen- and sulfur-containing functionalities on the catalyst surface (Table 1). Also, information about the presence and relative oxidation state of the active metal was collected. For all catalysts, the XPS C1s spectrum revealed a high amount of carbon functionalities (total C-% from 87 to 96%, see Table 1) on the surface, consisting mainly of carbon-carbon-type bonds and some carbon-oxygen functionalities. From the O1s pattern (Table 1, Fig. S3), both ACB and ACB2 catalysts were showing higher atomic percent for oxygen functionalities on the surface indicating surface oxidation. For ACB2 the oxygen content, ca. 12%, was higher than for ACB (ca. 6%, Table 1). From the O1s pattern, the signal at 531 eV can be assigned to C=O double bonds in carbonyl groups as well as to S=O double bonds in sulfonic acid groups. The peak at 533 eV can correspond to the single-bonded oxygen atoms, e.g., from hydroxyl groups of phenol type, or to S-O bonds e.g., in sulfonic acid groups [49-51]. In addition, the peak at 168 eV in the XPS spectra for S2p (Fig. S4) indicated the presence of sulfonic acid groups in both ACB and ACB2 [52]. The high-resolution XPS spectra of ACL and ACL2 (Fig. S4) for Zn2p showed peaks at 1022 eV, corresponding to $Zn2p_{3/2}$, and at 1045 eV assigned to $Zn2p_{1/2}$. This indicated the presence of zinc oxide (Zn^{2+}) in the catalysts [53], which was also in accordance with the XRD analysis. For ACW, the total amount of oxygen groups detected on the surface with XPS O1s scan was about 4%. This indicates the presence of for example carboxylic acid groups, which are common in the surfaces of activated carbons [27].

Table 1. Atomic percentages (atom-%) of surface groups based on the XPS analysis from catalysts obtained *via* binding energies of the C1s, O1s, S2p and Zn2p photoelectrons [32-35].

Sample	BE (eV)[a]	ACW % [b]	ACB % [b]	ACB2 % [b]	ACL % [b]	ACL2 % [b]
Total C-%	From C1s	95.7	93.4	87.4	95.4	94.5
C- (sp^3)	(284.8 eV)	52.2	49.7	43.0	51.9	50.6
C= (sp^2)	(285.7 eV)	25.2	25.8	26.5	25.6	25.7
C-O	(288.3 eV)	7.7	7.8	9.7	7.4	7.5
C=O	(290.9 eV)	8.1	7.7	6.3	8.0	8.3
π–π* in aromatic ring	(293.4 eV)	2.6	2.5	2.0	2.5	2.5
Total O-%	From O1s	4.3	6.3	12.4	3.9	4.6
O=	(531 eV)	2.2	1.3	3.7	2.4	3.2
O-	(533 eV)	2.1	4.3	7.6	1.2	1.0
H_2O (ads.)	(536 eV)	n.d.	0.6	1.2	0.3	0.4
Total S-%	(168 eV)	n.d.	0.2	0.1	n.d.	n.d.
Total Zn-%	(1022 eV)	n.d.	n.d.	n.d.	0.4	0.6

[a] binding energy ± 0.2 eV

[b] % is the relative amount from atom percent of the total sample

The total amount of acid sites on the surfaces of ACW, ACB, ACB2, ACL and ACL2 was determined by temperature-programmed desorption of ammonia (NH_3-TPD). The position and the area of the

desorption peak correlates directly with the acid strength and the acid amount, respectively. The desorption process of ammonia was measured up to 800 °C. From the TPD profiles (Fig. S5) desorption peaks at 700 °C for ACB2 and at 750 °C for ACL and ACL2 were detected. These high-temperature peaks can be attributed to the desorption of NH_3 from strong Brønsted acid sites with strong and broad desorption peak between 500 and 700 °C [54] and from more thermally stable strong Lewis acid sites at higher temperature, respectively [50, 55]. According to NH_3-TPD-performed analysis, ACW might contain some amount of acidic surface groups, up to a total of 0.45 mmol/g, which could originate from oxygen-bearing functionalities, e.g. carboxylic acids, anhydrides, lactones, lactols or phenols which are typical acidic groups on the activated carbon surface [27]. The number of total acid sites introduced into the catalysts was, at highest, 1.32 mmol/g when the AC was modified with 18 M H_2SO_4 (ACB2) and was three times higher than for ACW indicating addition of acidic functionalities on the surface. As expected, treatment with 9 M H_2SO_4 did not add acidity as much as the treatment with strong acid. In fact, the acidity of ACB was 0.45 mmol/g, the same as for ACW. It is very likely, that detected sulfur compounds on ACB (see ICP-OES and XPS) were composed from other type of sulfur groups than from acidic sulfonic groups. According to literature, a large number of oxidized functionalities such as phenolic and carboxylic acid groups can be created on the carbon surface during the sulfuric acid treatment [56-59]. This seems to be in line with the results in this study, since measured sulfur content seemed to be relatively low, but acidity was increased (ACB2). I.e. not only sulfonic acids were formed during the H_2SO_4 treatment but also other oxidized functionalities such as acidic phenolic and carboxylic groups, for example, were formed. Treatment with zinc chloride seemed to increase acidity slightly in the ACLs, since metal oxide (ZnO) was present as a Lewis acid site in the catalyst. The acidity determined by NH_3-TPD was slightly higher in ACL (0.75 mmol/g) than in the ACL2 catalyst (0.62 mmol/g). However, no significant differences were detected with acid sites in ACL and ACL2, confirming that the catalysts were almost identical.

To conclude the catalyst characterization results, ACB and ACB2 had sulfur-containing functionalities on the catalyst surface. Based on the NH_3-TPD analysis, sulfuric acid treatment with concentrated acid increased the acidity of the ACB2 catalyst. However, also other oxidized functionalities than sulfonic acids seemed to be present such as phenol or carboxylic acid groups increasing the acidic sites on the surface. With the characterization of ACL and ACL2, the addition of zinc was detected with STEM and ICP-OES analysis. Further, the metal phase as metal oxide (ZnO) was verified with XRD and XPS. Overall, both Lewis acid catalysts were almost identical, even though, the nominal metal content was different, indicating $ZnCl_2$ impregnation was not successful at higher loading. In the future, optimization of the preparation method of activated carbon catalysts containing Lewis and Brønsted acid sites still needs work to obtain higher acidic site loading on the catalyst.

3.2 Conversion of glucose into HMF

Prepared heterogeneous catalysts (ACW, ACB, ACB2, ACL, ACL2, ACBL and ACBL2) were used to convert glucose to HMF in biphasic media consisting of water and THF. A reaction temperature of 160 °C and a time of 8 hours, were chosen based on some preliminary experiments and were kept constant (Table 2). The first reaction was carried out without catalyst and only a 1% HMF yield was obtained, which indicated that the THF/water mixture could not catalyze the reaction by itself and acted only as a solvent (entry 1). Since THF and water are mutually miscible, NaCl was added to the reaction vessel in order to saturate the water phase and separate the layers. In the biphasic system, the produced HMF was extracted into THF *in situ*, hindering contact between HMF and water. This prevented HMF from reacting further into undesired byproducts. However, NaCl has been shown to catalyze HMF production, since the chloride ions enhance

the glucose to fructose isomerization step as well as the fructose to HMF dehydration step [60]. Therefore, another reference reaction with NaCl but without any other catalyst was performed, and a HMF yield of 35% was achieved (entry 2). The reaction selectivity was only 44%, though. When prepared catalysts were introduced to the reaction system, the HMF yield and the reaction selectivity increased. With ACW the yield increased by 9 percentage units to 44% (entry 3), which was probably due to the acidity of oxygen-containing groups on the surface of the ACW (XPS, Table 1). The reaction selectivity increased to 57%. When ACB, ACB2, ACL or ACL2 were used as the catalyst, the HMF yield increased to 46–49% (entries 4-7), indicating a slight increase compared to NaCl- and ACW-catalyzed reactions. ACB2 and ACL2 produced slightly higher HMF yields than ACB and ACL, but the difference was only 2 percentage units in both cases (entries 4-5 and 6-7). Based on catalyst characterization results, similar HMF yields between ACL and ACL2 were reasonable since their metal contents differed only by 0.1 wt.% according to ICP-OES, and 0.2 atom-% according to XPS. Also, similar HMF yields, 46% and 48%, achieved with ACB and ACB2 catalysts, respectively, were supported by the characterization results with XPS. HMF yields achieved with ACB and ACB2 were excellent compared to those described in the literature, where the isomerization step is not usually catalyzed successfully by acid-treated carbon catalysts [61]. It must be noted, though that NaCl was present in the reaction system and most likely took part in the isomerization of glucose to fructose [60]. Similar yields between ACB and ACL as well as between ACB2 and ACL2 (difference of only 1 percentage unit, entries 4–7) can also be explained by the effect of NaCl. Since the HMF yields achieved with ACL, ACL2, ACB and ACB2 catalysts were similar, the reaction selectivity was determined only for the reactions performed with ACB2 and ACL2 catalysts. Both catalysts functioned equally resulting in reaction selectivity of 67% (entries 5 and 7), which was 10 percentage units higher than with ACW. This indicated that even if the catalyst modification did not have a strong effect on the HMF yield, it increased the reaction selectivity considerably. However, the selectivity was not affected by whether the catalyst was modified with Lewis or Brønsted acid.

Creating tandem sites in the same AC catalyst is problematic because, after the sulfonation of AC, impregnating zinc in the catalyst without destroying the oxygen-bearing sulfonic acid groups is challenging, since high temperatures (> 250 °C) during the calcination process can destroy these sulfonic groups [62]. Therefore, two catalytic mixtures, ACBL and ACBL2, were prepared and used in the conversion reaction to introduce Brønsted and Lewis acid functionalities in the reaction system simultaneously. With ACBL as the catalyst, similar HMF yields (48%, entry 8) as those achieved with the ACB, ACB2, ACL, and ACL2 catalysts were generated. However, with ACBL2 as the catalyst, the HMF yield increased to 51% (entry 9). Also, the reaction selectivity increased further to 78% when compared to single acid catalysts ACB2 or ACL2. Therefore, based on the results, it seems that both Brønsted and Lewis acid sites not only accelerate the conversion reaction but also affect the reaction selectivity. The increase in HMF yield was not as high as expected (only 2 percentage units compared to ACL2) but the increase in reaction selectivity was significant (11 percentage units). In the literature, HMF yields of 63%, 53% and 23.1% and reaction selectivities of 63%, 60% and 24%, respectively, have been achieved in similar reaction media (water/THF/NaCl) with solid TiO_2-ZrO_2+Amberlyst 70, Sn-Beta with NH_4F and $FePO_4$ catalysts, respectively [22, 25, 63]. The HMF yield of 51% achieved in this study is comparable to those obtained in above mentioned studies and HMF selectivity of 78% is notably better compared to those. Also, the studied catalytic mixture was prepared using more sustainable lignocellulosic waste as a raw material for the catalysts support, thereby increasing the value of the obtained results.

The effect of solvent system was studied with the ACBL2 catalyst, which produced the highest HMF yield in previous reactions (Table 2). When the reaction was carried out in water, the HMF yield was low: 15% (entry 10). This indicates that although the biphasic system was important the lack of NaCl could have

attributed to the low HMF yield. Therefore, the reaction was repeated using NaCl. However, the HMF yield was even lower—only 10% (entry 11). Based on GC-MS spectra, it was concluded that notable amount of levulinic acid (14%) was formed when NaCl was introduced into the reaction and only water was used as the solvent. In the biphasic reactions, only trace amounts (< 4%) of levulinic acid were detected.

Finally, the studied ACB2, ACL2, and ACBL2 catalysts were compared to homogeneous catalysts, in which the amounts of H_2SO_4 and Zn were similar to those in heterogeneous catalysts. With homogeneous catalysts the HMF yields as well as the reaction selectivities were lower than with the studied AC-based catalysts, only 33–37% and 43-47%, respectively (entries 12–14). Low selectivities are consistent with literature since homogeneous catalysts and NaCl increase the production of soluble humins and humin precursors [64, 65, 50]. Low HMF yields are also reasonable since the amounts of H_2SO_4 and/or Zn were very low in homogeneous systems.

Table 2. Results for conversion of glucose to HMF using various catalysts and solutions.

Entry	System	Catalyst	HMF yield (%)	Selectivity (%)
1	water/THF	-	1	-
2	water/THF/NaCl	-	35	44
3	water/THF/NaCl	ACW	44	57
4	water/THF/NaCl	ACB	46	-
5	water/THF/NaCl	ACB2	48	67
6	water/THF/NaCl	ACL	47	-
7	water/THF/NaCl	ACL2	49	67
8	water/THF/NaCl	ACBL	48	-
9	water/THF/NaCl	ACBL2	51	78
10	water	ACBL2	15	-
11	water/NaCl	ACBL2	10	-
12	water/THF/NaCl	H_2SO_4[a]	37	47
13	water/THF/NaCl	$ZnCl_2$[b]	35	43
14	water/THF/NaCl	$H_2SO4 + ZnCl_2$[c]	33	45

Reaction conditions: 3 mg catalyst, 45 mg glucose, 0.35 g NaCl, 1 ml water, 3 ml THF, 160 °C, 8 h. [a] 1.944 mM H_2SO_4 (corresponding to 3 mg ACB2), [b] 0.1158 g/l $ZnCl_2$ (corresponding to 3 mg ACL2), [c] 0.972 mM H_2SO_4 and 0.0579 g/l $ZnCl_2$ (corresponding to 3 mg ACBL2).

The results from the glucose to HMF conversion reactions suggested that activated carbon itself had an important role as a catalyst during the reaction. Based on the catalyst characterizations the amounts of Lewis and Brønsted acid sites were low in heterogeneous catalysts, so it is likely that activated carbon's high specific surface area and oxygen-containing surface groups had an impact on its catalytic activity. These groups might participate in the dehydration reaction of fructose to HMF, while the large surface area of activated carbon may promote the conversion of glucose by increasing contact areas between reactants [26, 29]. Besides this study, there are also several examples in the literature of how the surface of activated carbon plays an important role in catalytic reactions, such as alcohol dehydration [27, 66, 67]. However, from the reaction selectivity point of view the values achieved in this study with plain water washed activated carbon were considerably lower than those with acid treated carbon catalysts.

3.2.1 Optimization of reaction time and catalyst loading

ACBL2 was chosen for optimization experiments because it produced the highest HMF yield compared to the other catalysts (Table 2). The same reaction temperature, 160 °C, and a biphasic water:THF system were used as in previous reactions, but the reaction time and catalyst loading were varied in order to find the optimal reaction conditions for the conversion of glucose to HMF. As shown in Figure 3a, the HMF yield increased from 8% to 51% when the reaction time increased from 1 to 8 hours, respectively. With a longer reaction time, the HMF yield started to decrease, indicating that 8 hours was the optimal time to maximize the yield. In addition, the amount of 1,4-butanediol, which is the degradation product of THF, was observed to increase with the increasing reaction time. However, the most significant increase in the amount of 1,4-butanediol occurred when the reaction time was 10 hours, implying that 8 hours may be the optimal reaction time also regarding the stability of the biphasic system. The amount of levulinic acid did not seem to increase with increasing time, which implied that the biphasic system worked successfully and prevented rehydration of HMF in the organic phase.

The amount of catalyst was varied in the range of 1.5–18 mg to determine the optimal catalyst loading. As shown in Figure 3b, the catalyst amount of 1.5 mg was clearly too low to accelerate the conversion reaction, but when the amount was increased to 3 mg, the HMF yield improved significantly, from 45 to 51%. When the catalyst loading was increased to 9 mg, the increase in the HMF yield was only 2 percentage units. A further increase in the catalyst amount caused the HMF yield to decrease (Figure 3b), which may be due to the higher amount of Brønsted acid or metal sites in the reaction system, which accelerated side reactions. This was confirmed by measuring levulinic acid concentrations, which increased together with the catalyst loading (Figure 3b). It was also noticed that the formation of 1,4-butanediol in the THF phase was increased with increasing amounts of catalyst. In addition to levulinic acid and 1,4-butanediol, some other unidentified byproducts were formed when the catalyst loading was increased. Thus, 3 mg was selected as the optimal amount of catalyst for the conversion reaction, providing a high yield of HMF with a low amount of byproducts.

Figure 3. (a) Effect of reaction time on HMF yield. (b) Effect of catalyst loading on HMF and levulinic acid (LA) yield.

3.2.3 Preliminary recycling experiments

The recyclability of the catalyst is of great importance in the practical production of HMF. In this study, the catalyst was recycled together with the whole water phase, because the separation of the catalyst would have significantly reduced the amount of catalyst. The analysis of water phases from previous reactions revealed that the water phase was suitable for recycling since it did not contain significant amounts of byproducts: only HMF (yield 5–7%), gamma-butyrolactone and 1,4-butanediol were detected. Also, unreacted glucose (ca. 34%) was present in the water phase after the conversion reactions, which was taken into account during the subsequent runs.

Recycling was accomplished with an 8-hour reaction time and a 3-mg dosage of ACBL2 catalyst. After the first reaction the organic phase was removed and analyzed for the HMF yield and a fresh portion of glucose and THF was added among the water phase for the next run. The results of the recycling experiments are shown in Figure 4 and based on them the HMF yield decreased after each consecutive run. However, the decrease in the yield was not significant until after the third run, when it was over 20%. After that the yield seemed to balance and decreased only slightly between fourth and fifth run. The decrease in

the yield during the recycling experiments could have been caused by adsorption and accumulation of polymeric side products or humins on the acid sites in the porous catalyst [68]. The composition of the THF layer did not change notably during the first four runs. After fifth run byproducts such as levulinic acid and 2,3-dihydro-3,5-dihydroxy-6-methyl-4(H)-pyran-4-one [69] were detected with GC-MS. This indicates that HMF was successfully isolated along with the organic phase between the runs.

Figure 4. The normalized HMF yield after each recycling run in relation to the first run.

4. Conclusions

Lignocellulosic waste material, birch sawdust, was used as a raw material for the preparation of activated carbon based catalysts. The prepared novel catalysts, ACB, ACB2, ACL, and ACL2, were characterized extensively and found to contain Lewis or Brønsted acid sites on the catalyst surface. Catalysts were used in water:THF biphasic system to convert glucose to HMF. The highest HMF yield and selectivity, 51% and 78%, respectively, were obtained with the mixture of ACB2 and ACL2. Also, ACW produced good HMF yield, 44%, but the selectivity was only 57%. The prepared heterogeneous catalysts were found to be more effective than homogeneous sulfuric acid or $ZnCl_2$, indicating that activated carbon based catalysts are promising for HMF production, especially in terms of reaction selectivity.

Acknowledgement
The authors acknowledge Davide Bergna for preparing the activated carbon, Seija Liikanen for ICP-OES measurements and Zouhair El Assal for TPD measurements. Also, the Center of Microscopy and Nanotechnology at the University of Oulu is acknowledged for their facilities for STEM/EFTEM imaging and XPS and XRD measurements.

Funding
This work was supported by two projects of the EU/European Regional Development Fund, leveraged from the EU program: project Biomass value chains (no. A71029) and project PreBio (no. A70594). The financial support of EU/Interreg Botnia-Atlantica for project Green Bioraff Solutions (no. 20201508) and Fortum foundation (201700072) is also greatly acknowledged.

Declarations of interest: none.

References

[1] S.P. Teong, G. Yi, Y. Zhang, Green Chem. 16 (2014) 2015-2026.

[2] I.K.M. Yu, D.C.W. Tsang, Bioresour. Technol. 238 (2017) 716-732.

[3] T. Wang, M.W. Nolte, B.H. Shanks, Green Chem. 16 (2014) 548-572.

[4] L.T. Mika, E. Cséfalvay, Á Németh, Chem. Rev. 118 (2018) 505-613.

[5] C. Moreau, R. Durand, S. Razigade, J. Duhamet, P. Faugeras, P. Rivalier, R. Pierre, G. Avignon, Appl. Catal. A Gen. 145 (1996) 211-224.

[6] M.J. Antal, W.S. Mok, G.N. Richards, Carbohydr. Res. 199 (1990) 91-109.

[7] Y. Qu, C. Huang, J. Zhang, B. Chen, Bioresour. Technol. 106 (2012) 170-172.

[8] F.K. Kazi, A.D. Patel, J.C. Serrano-Ruiz, J.A. Dumesic, R.P. Anex, Chem. Eng. J. 169 (2011) 329-338.

[9] Y. Román-Leshkov, J.N. Chheda, J.A. Dumesic, Science 312 (2006) 1933-1937.

[10] J. Zhang, E. Weitz, ACS Catal. 2 (2012) 1211-1218.

[11] J. Lewkowski, ARKIVOC 2001 (2005) 17-54.

[12] B. Saha, M.M. Abu-Omar, Green Chem. 16 (2014) 24-38.

[13] D. Chen, F. Liang, D. Feng, M. Xian, H. Zhang, H. Liu, F. Du, Chem. Eng. J. 300 (2016) 177-184.

[14] R. van Putten, van der Waal, Jan C, E. de Jong, C.B. Rasrendra, H.J. Heeres, J.G. de Vries, Chem. Rev. 113 (2013) 1499-1597.

[15] C.J. Moye, Rev. Pure Appl. Chem. 14 (1964) 161-170.

[16] M.S. Feather, J.F. Harris, Adv. Carbohydr. Chem. 28 (1973) 161-224.

[17] P. Bhaumik, P.L. Dhepe, Catal. Rev. 58 (2016) 36-112.

[18] B.Y. Yang, R. Montgomery, Carbohydr. Res. 280 (1996) 27-45.

[19] Y. Yang, C. Hu, M.M. Abu-Omar, Green Chem. 14 (2012) 509-513.

[20] Y.J. Pagán-Torres, T. Wang, J.M.R. Gallo, B.H. Shanks, J.A. Dumesic, ACS Catal. 2 (2012) 930-934.

[21] P.Y. Dapsens, C. Mondelli, J. Pérez-Ramírez, ACS Catal. 2 (2012) 1487-1499.

[22] L. Atanda, A. Silahua, S. Mukundan, A. Shrotri, G. Torres-Torres, J. Beltramini, RSC Adv. 5 (2015) 80346-80352.

[23] X. Wang, H. Zhang, J. Ma, Z. Ma, RSC Adv. 6 (2016) 43152-43158.

[24] J.M.R. Gallo, D.M. Alonso, M.A. Mellmer, J.A. Dumesic, Green Chem. 15 (2012) 85-90.

[25] G. Yang, C. Wang, G. Lyu, L.A. Lucia, J. Chen, BioResources 10 (2015) 5863-5875.

[26] F. Rodríguez-Reinoso, Carbon 36 (1998) 159-175.

[27] J.L. Figueiredo, M.F.R. Pereira, Catal Today 150 (2010) 2-7.

[28] T.J. Bandosz, Surface Chemistry of Carbon Materials, in: P. Serp, J.L. Figueiredo (Eds.), Carbon Materials for Catalysis, John Wiley & Sons, 2008, pp. 45-92.

[29] E. Lam, J.H.T. Luong, ACS Catal. 4 (2014) 3393-3410.

[30] J.L. Figueiredo, M.F.R. Pereira, M.M.A. Freitas, J.J.M. Órfão, Carbon 37 (1999) 1379-1389.

[31] C. Moreno-Castilla, M.V. López-Ramón, F. Carrasco-Marín, Carbon 38 (2000) 1995-2001.

[32] Y. Yang, K. Chiang, N. Burke, Catal. Today 178 (2011) 197-205.

[33] Anon., Calgon Carbon Corporation Investor Presentation, 2011, http:// phx.corporate-ir.net/External.File?item=UGFyZW50SUQ9ODc0MjV8Q2hpbGRJRD0tMXxUeXBlPTM=& t=1, accessed 19 September 2018.

[34] M. Danish, T. Ahmad, Renew. Sust. Energ. Rev. 87 (2018) 1-21.

[35] L. Prati, D. Bergna, A. Villa, P. Spontoni, C.L. Bianchi, T. Hu, H. Romar, U. Lassi, Catal. Today 301 (2018) 239-243.

[36] P. González-García, Renew. Sust. Energ. Rev. 82 (2018) 1393-1414.

[37] T. Deng, J. Li, Q. Yang, Y. Yang, G. Lv, Y. Yao, L. Qin, X. Zhao, X. Cui, X. Hou, RSC Adv. 6 (2016) 30160-30165.

[38] X. Xiong, I.K.M. Yu, S.S. Chen, D.C.W. Tsang, L. Cao, H. Song, E.E. Kwon, Y.S. Ok, S. Zhang, C.S. Poon, Catal. Today 314 (2018) 52-61.

[39] B. Zou, X. Chen, C. Zhou, X. Yu, H. Ma, J. Zhao, X. Bao, Can. J. Chem. Eng. 96 (2018) 1337-1344.

[40] N.I. Villanueva, T.G. Marzialetti, Catal. Today 302 (2018) 100-107.

[41] U. Tyagi, N. Anand, D. Kumar, Bioresour. Technol. 267 (2018) 326-332.

[42] J.H. Clark, V. Budarin, T. Dugmore, R. Luque, D.J. Macquarrie, V. Strelko, Catal. Commun. 9 (2008) 1709-1714.

[43] E. Mäkelä, R. Lahti, S. Jaatinen, H. Romar, T. Hu, R.L. Puurunen, U. Lassi, R. Karinen, ChemCatChem 10 (2018) 3269-3283.

[44] R. Lahti, D. Bergna, H. Romar, T. Hu, A. Comazzi, C. Pirola, C.L. Bianchi, U. Lassi, Top. Catal. 60 (2017) 1415-1428.

[45] S. Brunauer, P.H. Emmett, E. Teller, J. Am. Chem. Soc. 60 (1938) 309-319.

[46] N.A. Seaton, Walton, J. P. R. B., N. Quirke, Carbon 27 (1989) 853-861.

[47] W.T. Tsai, C.Y. Chang, S.L. Lee, S.Y. Wang, J. Therm. Anal. Cal. 63 (2001) 351–357.

[48] S.A. Schmidt, N. Kumar, A. Shchukarev, K. Eränen, J-P. Mikkola, D.Y. Murzin, T. Salmi, Appl. Catal., A 468 (2013) 120-134.

[49] P. Rechnia-Goracy, A. Malaika, M. Kozlowski, Diamond Relat. Mat. 87 (2018) 124-133.

[50] P.P. Upare, J. Yoon, M.Y. Kim, H. Kang, D.W. Hwang, Y.K. Hwang, H.H. Kung, J. Chang, Green Chem. 15 (2013) 2935-2943.

[51] P. Burg, P. Fydrych, D. Cagniant, G. Nanse, J. Bimer, A. Jankowska, Carbon 40 (2002) 1521-1531.

[52] Q. Shu, J. Gao, Z. Nawaz, Y. Liao, D. Wang, J. Wang, Appl. Energy 87 (2010) 2589-2596.

[53] C.H. Kim, B.H. Kim, J. Power Sources. 274 (2015) 512-520.

[54] M. Farabi, M. Ibrahim, U. Rashid, Y. Taufiq-Yap, Energy Convers. Manag. 181 (2019) 562-570.

[55] F. Lónyi, J. Valyon, Micropor. Mesopor. Mater. 47 (2001) 293-301.

[56] J. Wang, W. Xu, J. Ren, X. Liu, G. Lua, Y. Wang, Green Chem. 13 (2011) 2678-2681.

[57] S. Kang, J. Ye, Y. Zhanga, J. Chang, RSC Adv. 3 (2013) 7360-7366.

[58] H.T. Gomes, S.M. Miranda, M.J. Sampaio, J.L. Figueiredo, A.M.T. Silva, J.L. Faria, Appl. Catal. B: Environ., 106 (2011) 390-397.

[59] X. Xiong, I.K.M. Yu, S.S. Chen, D.C.W. Tsang, L. Cao, H. Song, E.E. Kwon, Y.S. Ok, S. Zhang, C.S. Poon, Catal. Today, 314 (2018) 52-61.

[60] X. Li, Y. Zhang, Q. Xia, X. Liu, K. Peng, S. Yang, Y. Wang, Ind. Eng. Chem. Res. 57 (2018) 3545-3553.

[61] W. Daengprasert, P. Boonnoun, N. Laosiripojana, M. Goto, A. Shotipruk, Ind. Eng. Chem. Res. 50 (2011) 7903-7910.

[62] Q. Pang, L. Wang, H. Yang, L. Jia, X. Pan, C. Qiu, RSC Adv. 4 (2014) 41212-41218.

[63] L. Yang, X. Yan, S. Xu, H. Chen, H. Xia, S. Zuo, RSC Adv. 5 (2015) 19900-19906.

[64] V. Maruani, S. Narayanin-Richenapin, E. Framery, B. Andrioletti, ACS Sustainable Chem. Eng. 6 (2018) 13487-13493.

[65] I.K.M Yu, D.C.W Tsang, Bioresour. Technol. 238 (2017) 716-732.

[66] Q.X. Lin, C.H. Zhang, X.H. Wang, B.G. Cheng, N. Mai, J.L. Ren, Catal. Today (2018) Article in press.

[67] S.S. Chen, T. Maneerung, D.C.W. Tsang, Y.S. Ok, C.H. Wang, Chem. Eng. J. 328 (2017) 246-273.

[68] A. Deng, Q. Lin, Y. Yan, H. Li, J. Ren, C. Liu, R. Sun, Bioresour. Technol. 216 (2016) 754-760.

[69] M. Kim, W. Baltes, J. Agric. Food Chem. 44 (1996) 282-289.

Figures

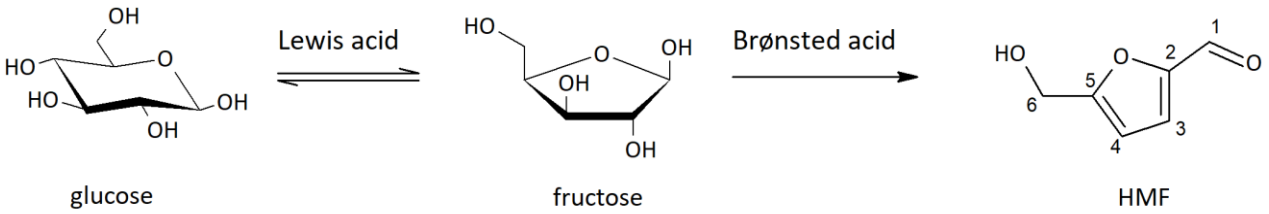

Figure 1. General reaction scheme of HMF formation from glucose. First glucose is isomerized into fructose over Lewis acid catalyst and then fructose is dehydrated into HMF over Brønsted acid catalyst.

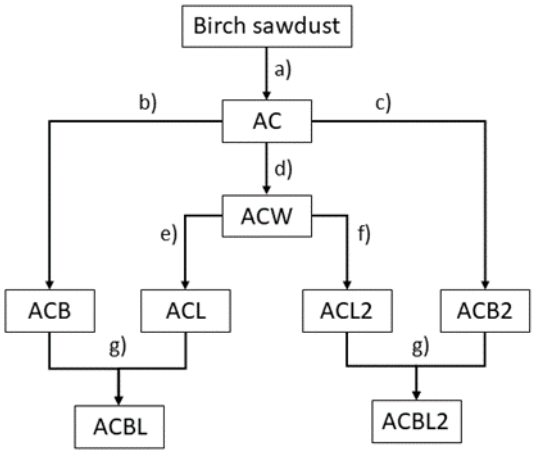

Figure 2. Flow chart for catalyst preparation: a) carbonization and activation step b) acid modification with 9 M H_2SO_4 c) acid modification with 18 M H_2SO_4 d) washing with H_2O e) impregnation with $ZnCl_2$ (5 wt.% Zn) f) impregnation with $ZnCl_2$ (15 wt.% Zn) g) mixing in 1:1 ratio.

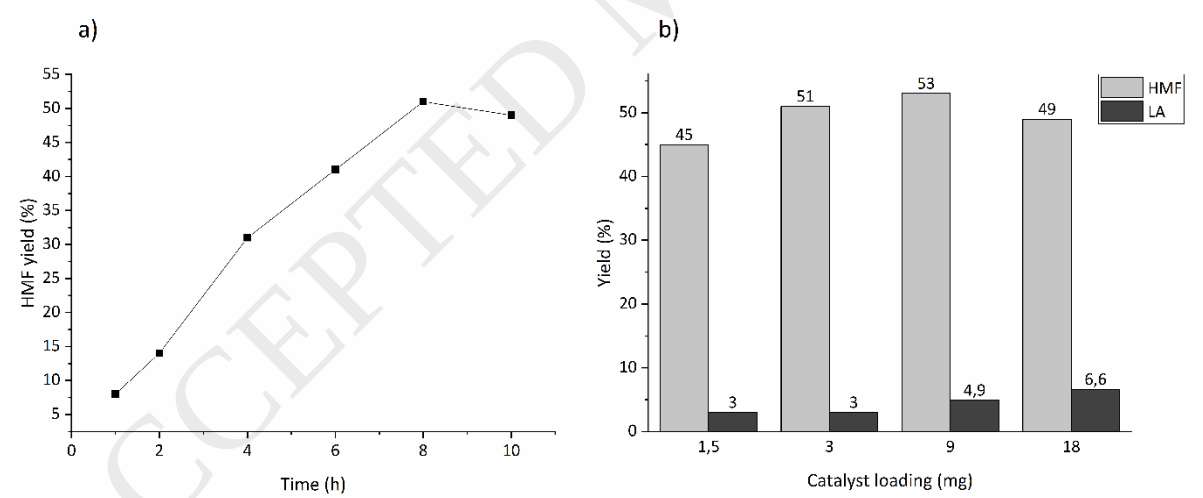

Figure 3. a) Effect of reaction time on HMF yield. b) Effect of catalyst loading on HMF and levulinic acid (LA) yield.

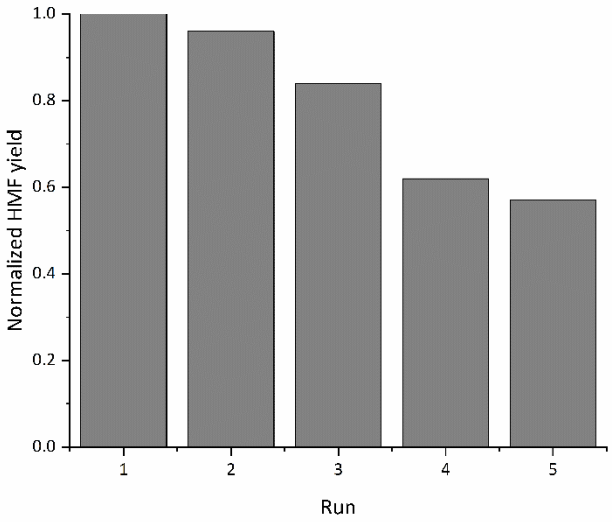

Figure 4. The normalized HMF yield after each recycling run in relation to the first run.